Inorg. Chem. **2002**, *41*, 5269–5275

Phosphine and Phosphonite Complexes of a Ru(II) Porphyrin. 2. Photophysical and Electrochemical Studies

Eugen Stulz,[†] Jeremy K. M. Sanders,*[,†] Marco Montalti,[‡] Luca Prodi,*[,‡] Nelsi Zaccheroni,[‡] Fabrizia Fabrizi de Biani,[§] Emanuela Grigiotti,[§] and Piero Zanello*[,§]

University Chemical Laboratory, University of Cambridge, Lensfield Road, Cambridge, CB2 1EW, U.K., Università di Bologna, Dipartimento di Chimica "G. Ciamician", Via Selmi 2, 40126 Bologna, Italy, and Università degli Studi di Siena, Dipartimento di Chimica, Via A. Moro, 53100 Siena, Italy

Received May 17, 2002

The photophysical and electrochemical properties of a series of mono- and bis-phosphine complexes of a 5,15-diphenyl-substituted ruthenium porphyrin, (MeOH)Ru^{II}(CO)(DPP) **1**, were investigated. The ligands used were diphenyl(phenylacetenyl)phosphine (DPAP), diethyl (phenylacetenyl)phosphonite [PAP(OEt)$_2$], tris(phenylacetenyl)phosphine [(PA)$_3$P], and bis(diphenylphosphino)acetylene (DPPA). All complexes display two reversible one-electron oxidations at: 0.61 and 1.0 V vs SCE (**1**), 0.42–0.51 and 0.97–1.05 V [(PR$_3$)Ru^{II}(CO)(DPP)], and 0.06–0.25 and 0.82–0.95 V [(PR$_3$)$_2$Ru^{II}(DPP)]. As predicted by EHMO calculations, the first oxidation is porphyrin or phosphorus centered, whereas the second one is ruthenium centered. Bulk electrolysis at the first oxidation potential yields stable monocations. Simulation of the cyclic voltammogram of (DPAP)Ru^{II}(CO)(DPP) in CH_2Cl_2 demonstrates the kinetic lability of the complex, and the association constant found ($K = 1.27 \times 10^6$ M^{-1}) is in accordance with the value determined by UV–vis titration ($K = 1.2 \pm 0.3 \times 10^6$ M^{-1}). Coordination of one phosphine ligand to Ru^{II}(CO)(DPP) leads to a red shift in both the absorption and luminescence spectra. Shifts are typically 10 nm for the B- and Q-band absorptions and are not affected by the nature of the phosphorus ligand. The intense luminescence of (PR$_3$)Ru^{II}(CO)(DPP), red-shifted by 21–28 nm compared to **1**, can be attributed to originate from a $^3(\pi,\pi^*)$ excited state, and it exhibits lifetimes from 150 to 240 μs. In the bis-phosphine complexes (PR$_3$)$_2$Ru^{II}(DPP), the Q-band absorption is broadened and does not show any distinct peak. Judged from EHMO calculation, this could arise from a low-energy charge-transfer state involving the phosphorus ligand. The luminescence is efficiently quenched due to radiationless decay from a charge-transfer excited state, involving either the metal center or the phosphorus ligand; an unambiguous assignment could not be made.

Introduction

Recently, we have shown that phosphine-substituted porphyrins are versatile building blocks for the construction of supramolecular assemblies.[1] In view of possible photophysical applications, the use of phosphorus to connect porphyrins via coordination chemistry to ruthenium(II), together with the immense diversity accessible by the variation of the substituents on the coordinating phosphorus, should offer a convenient means for fine-tuning the physical properties of the assemblies. In order to predict electronic interactions in multiporphyrinic arrays, it is essential to have detailed knowledge about the structure and physical properties of phosphorus metalloporphyrin complexes. In the preceding paper,[2] we described the synthesis of mono- and bis-phosphorus ruthenium(II) porphyrin complexes. The studies were concerned with the solution chemistry and the solid state structure of the complexes. In particular, we examined the influence of the stereoelectronic properties of the ligands on NMR and IR spectroscopy and on the stability of the complexes in solution. In this study, we were interested

* To whom correspondence should be addressed. E-mail: jkms@cam.ac.uk (J.K.M.S.); lprodi@ciam.unibo.it (L.P.); zanello@unisi.it (P.Z.).
[†] University of Cambridge.
[‡] Università di Bologna.
[§] Università degli Studi di Siena.

(1) (a) Darling, S. L.; Stulz, E.; Feeder, N.; Bampos, N.; Sanders, J. K. M. *New J. Chem.* **2000**, *24*, 261. (b) Stulz, E.; Ng, Y.-F.; Scott, S. M.; Sanders, J. K. M. *Chem. Commun.* **2002**, 524.

(2) Stulz, E.; Maue, M.; Feeder, N.; Teat, S. J.; Ng, Y.-F.; Bond, A. D.; Darling, S. L.; Sanders, J. K. M. *Inorg. Chem.* **2002**, *41*, 5255.

10.1021/ic025728q CCC: $22.00
Published on Web 09/12/2002

in the influence of the nature of the ligand on the photophysical and electrochemical behavior of $Ru^{II}(CO)(DPP)$ phosphorus complexes.

Generally, the photophysical and electrochemical properties of porphyrins and of their metalated derivatives are determined by the relative energies of the π molecular orbitals (a_{1u} and a_{2u}) of the macrocyle and the d-orbital levels of the central metal. These relative energies can be tuned to a significant degree, either by varying the peripheral substituents on the porphyrin,[3−5] by varying the central metal,[6,7] or by changing axial ligands bound to the central metal.[4,7−9] From Holten's study,[9] it is known that axial ligands significantly influence the physical properties of Ru(II) porphyrins. Of central importance is the CO ligand, which stabilizes the +2 state of the ruthenium due to its strong π-acid characteristics, thus lowering the dπ(Ru) orbital levels.[10] The sixth coordination site can be occupied by a variety of σ-donor and π-acceptor ligands; the strength of their coordination is strongly influenced by the presence or absence of the trans CO. Complexes of the form $(L)Ru^{II}(CO)(por)$ (por = porphyrin) exhibit phosphorescence from the lowest excited state, assigned as $^3(\pi,\pi^*)$.[9] This excited state is accessible via efficient $S_1 \rightarrow T_1$ intersystem crossing; the lifetimes of these triplet excited states are in the range of tens to hundreds of microseconds.[5] Complexes of the composition $(L)_2Ru^{II}(por)$ do not show room temperature luminescence due to radiationless decay from a (d,π^*) CT lowest excited state, exhibiting lifetimes in the order of tens of nanoseconds.[11] The effects are only marginally influenced by σ-donor ligands (pip, py, EtOH, PEt_3).

In $(L)Ru^{II}(CO)(por)$, the first reversible one-electron oxidation is usually porphyrin ring centered and arises from the $a_{1u}(\pi)$ or $a_{2u}(\pi)$ MO.[5,12] A second one-electron oxidation can be found at higher potential values and is assigned to the $Ru^{III/II}$ couple to form a Ru(III)−cation radical complex.[5,13] In contrast, loss of CO in $(L)_2Ru^{II}(por)$ complexes causes a cathodic shift of the metal-centered redox process, due to the absence of π-back-bonding.[10] Thus, the dπ(Ru) orbitals are the highest filled levels,[10,11] and the first oxidation corresponds to the $Ru^{III/II}$ couple. The second and third are assigned to the $Ru^{IV/III}$ and porphyrin-centered oxidations, but an assignment cannot be made unambiguously.[14] In both types of complexes, reduction processes occur at rather negative potential values.[15]

Chart 1

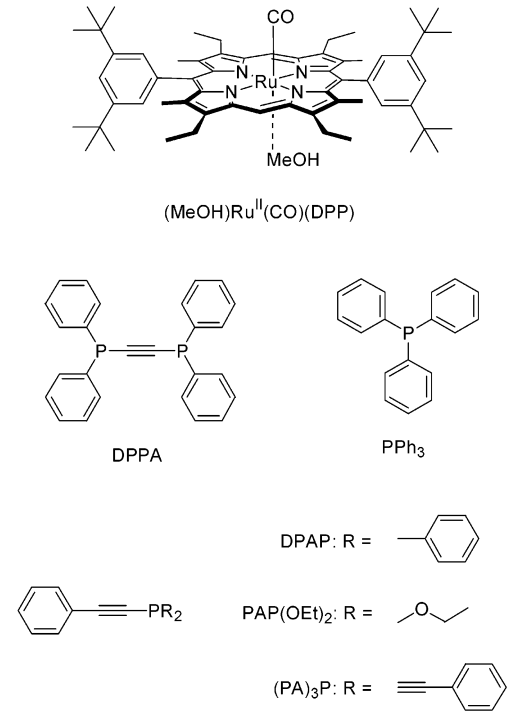

In this paper, we describe the absorption and emission spectroscopy, electrochemical behavior, and EHMO calculations of different phosphorus ruthenium porphyrin complexes (Chart 1). This study will help to elucidate the influence of different ligands on the physicochemical behavior of specific ruthenium(II) porphyrin complexes.

Experimental Section

Electrochemistry. $(MeOH)Ru^{II}(CO)(DPP)$, the phosphorus ligands, the mono-phosphorus complexes $(PR_3)Ru(CO)(DPP)$, and the bis-phosphorus complexes $(PR_3)_2Ru^{II}(DPP)$ were obtained as described in the preceding paper.[2] Anhydrous 99.9% (HPLC grade) dichloromethane (CH_2Cl_2) was obtained fom Aldrich. Electrochemical grade $[NBu_4][PF_6]$ supporting electrolyte was purchased from Fluka and used as obtained. All measurements were made in CH_2Cl_2 solution.

Cyclic voltammetry was performed in a three-electrode cell containing a platinum working electrode surrounded by a platinum-spiral counter electrode, and an aqueous saturated calomel reference electrode (SCE) mounted with a Luggin capillary. A BAS 100W electrochemical analyzer was used as polarizing unit. Controlled potential coulometry was performed in an H-shaped cell with anodic and cathodic compartments separated by a sintered-glass disk. The working macroelectrode was a platinum gauze; a mercury pool was used as the counter electrode. All the potential values are referred to the saturated calomel electrode (SCE). Under the experimental

(3) (a) Shediac, R.; Gray, M. H. B.; Uyeda, H. T.; Johnson, R. C.; Hupp, J. T.; Angiolillo, P. J.; Therien, M. J. *J. Am. Chem. Soc.* **2000**, *122*, 7017. (b) Vannelli, T. A.; Karpishin, T. B. *Inorg. Chem.* **2000**, *39*, 340. (c) Rovira, C.; Kunc, K.; Hutter, J.; Parrinello, M. *Inorg. Chem.* **2001**, *40*, 11.
(4) Cheng, R. J.; Chen, P. Y. *Chem.−Eur. J.* **1999**, *5*, 1708.
(5) Rillema, D. P.; Nagle, J. K.; Barringer, L. F.; Meyer, T. J. *J. Am. Chem. Soc.* **1981**, *103*, 56.
(6) Guldi, D. M.; Mody, T. D.; Gerasimchuk, N. N.; Magda, D.; Sessler, J. L. *J. Am. Chem. Soc.* **2000**, *122*, 8289.
(7) Kalyanasundaram, K. *Photochemistry of Polypyridine and Porphyrin Complexes*; Academic Press: London, 1992.
(8) Pilard, M. A.; Guillemot, M.; Toupet, L.; Jordanov, J.; Simonneaux, G. *Inorg. Chem.* **1997**, *36*, 6307.
(9) Levine, L. M. A.; Holten, D. *J. Phys. Chem.* **1988**, *92*, 714.
(10) Brown, G. M.; Hopf, F. R.; Ferguson, J. A.; Meyer, T. J.; Whitten, D. G. *J. Am. Chem. Soc.* **1973**, *95*, 5939.
(11) Young, R. C.; Nagle, J. K.; Meyer, T. J.; Whitten, D. G., *J. Am. Chem. Soc.* **1978**, *100*, 4773.
(12) Kadish, K. M.; Hu, Y.; Tagliatesta, P.; Boschi, T. *J. Chem. Soc., Dalton Trans.* **1993**, 1167.
(13) Lee, F. W.; Choi, M. Y.; Cheung, K. K.; Che, C. M. *J. Organomet. Chem.* **2000**, *595*, 114.
(14) Offord, D. A.; Sachs, S. B.; Ennis, M. S.; Eberspacher, T. A.; Griffin, J. H.; Chidsey, C. E. D.; Collman, J. P. *J. Am. Chem. Soc.* **1998**, *120*, 4478.
(15) Da Ros, T.; Prato, M.; Carano, M.; Ceroni, P.; Paolucci, F.; Roffia, S.; Valli, L.; Guldi, D. M. *J. Organomet. Chem.* **2000**, *599*, 62.

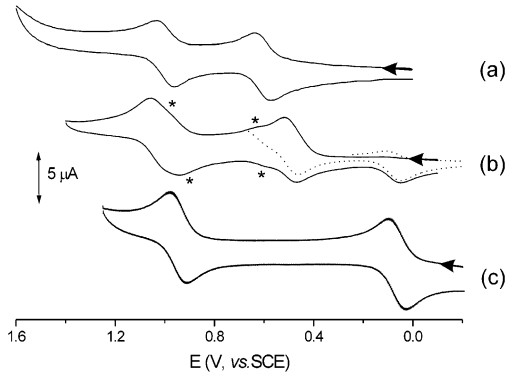

Figure 1. Cyclic voltammetry responses recorded at platinum electrode in CH_2Cl_2 solutions containing $[NBu_4][PF_6]$ (0.2 mol dm^{-3}): (a) (MeOH)-Ru^{II}(CO)(DPP) (0.3×10^{-3} mol dm^{-3}); (b) (DPAP)Ru^{II}(CO)(DPP) (0.1×10^{-3} mol dm^{-3}); (c) $(DPAP)_2Ru^{II}$(DPP) (0.3×10^{-3} mol dm^{-3}); scan rate 0.2 V s^{-1}. The dotted line shows the voltammogram obtained by inverting the scan after the first oxidation. The asterisks (*) indicate traces of (MeOH)-Ru^{II}(CO)(DPP) present in the sample.

conditions, the one-electron oxidation of ferrocene occurs at $E^{\circ\prime} = +0.39$ V. All the mono-phosphorus complexes were prepared in situ by mixing an equimolar amount of ligand to a deaerated (N_2-saturated) solution of (MeOH)Ru^{II}(CO)(DPP) in CH_2Cl_2. The reaction was monitored by cyclic voltammetry, the measurements being periodically repeated until the response remained unchanged.

Photophysical Studies. Photophysical experiments were conducted in 1×10^{-5} to 1×10^{-4} M CH_2Cl_2 solution at room temperature, and in an opaque rigid CH_2Cl_2 matrix for low-temperature (77 K) luminescence measurements. Absorption spectra were recorded with a Perkin-Elmer Lambda 16 spectrophotometer. Uncorrected emission spectra, corrected excitation spectra, and phosphorescence lifetimes were obtained with a Perkin-Elmer LS50 spectrofluorimeter. Emission spectra in a CH_2Cl_2 rigid matrix at 77 K were recorded using quartz tubes immersed in a quartz Dewar filled with liquid nitrogen. Corrections for instrumental response, inner filter effects, and phototube sensitivity were performed as previously described.[16]

Extended Hückel Calculations. EHMO calculations were performed by using the program CACAO.[17] The energy parameters obtained by DFT calculations[18] were used, while the exponential parts were taken from ref 19. The structural data employed to construct the molecular models are average values of experimental parameters derived from the Cambridge Crystallographic Data Centre.[23]

Results and Discussion

Electrochemical Properties. Figure 1 compares the cyclic voltammetric behavior of the unsubstituted precursor (MeO-H)Ru^{II}(CO)(DPP) with those of the mono-phosphine complex (DPAP)Ru^{II}(CO)(DPP) and the bis-phosphine complex $(DPAP)_2Ru^{II}$(DPP). The relative formal electrode potentials for all the redox processes are compiled in Table 1.

(MeOH)Ru^{II}(CO)(DPP) exhibits two subsequent one-electron oxidations, both possessing features of chemical and electrochemical reversibility (i_{pc}/i_{pa} constantly equal to 1; ΔE_p close to 60 mV), Figure 1a. An irreversible reduction process is also present at very negative potential values close to the solvent discharge. Controlled potential coulometry in correspondence to the first anodic process ($E_w = +0.7$ V) showed the consumption of one electron/molecule. On bulk oxidation the red/orange solution turns green and the stable cation $[Ru^{II}(CO)(DPP)]^+$ forms, as proved by the cyclic voltammograms which appear complementary to the original ones.

The mono-phosphine complex also exhibits two separate oxidation processes, displaying features of partial chemical reversibility, Figure 1b. Also in this case, a chemically irreversible reduction process is present at potential values almost overlapping the solvent discharge. Apart from minor traces of the (MeOH)Ru^{II}(CO)(DPP) precursor present in the solution (Figure 1b, starred peaks), it is evident that inverting the potential scan just after traversing the first oxidation process generates a new peak system at less positive potential value, which can confidently be assigned to $[(PR_3)_2Ru^{II/III}$-(DPP)$]^{0/+}$, as discussed below.

The bis-phosphine complex $(DPAP)_2Ru^{II}$(DPP) undergoes two chemically reversible one-electron oxidation processes, Figure 1c, which are notably separated with respect to the corresponding processes of either the ruthenium porphyrin precursor or the monophosphine complex. No reduction process was detected for complexes $(PR_3)_2Ru^{II}$(DPP). Upon controlled potential coulometry at $E_w = +0.2$ V, corresponding to the first oxidation of the complex, the red/orange solution turns brown. The fully oxidized solution displays cyclic voltammetric profiles complementary to the original ones, thus indicating the complete stability of the electrogenerated monocation.

The electrochemical behavior of the remaining bis-phosphorus complexes (L = $(PA)_3P$, $PAP(OEt)_2$) is essentially similar to that of the DPAP complex, except for L = DPPA. As shown in Figure 2, $(DPPA)_2Ru^{II}$(DPP) undergoes three oxidation processes, the second of which is irreversible in character. The electrogenerated cation $[(PAP(OEt)_2)_2Ru^{II}(DPP)]^+$ proved to be unstable in the long time scale of macroelectrolysis.

Returning to the cyclic voltammetric behavior of (PR_3)-Ru^{II}(CO)(DPP), the chemical path following the first oxidation is further supported by digital simulation of its cyclic voltammetric profiles. Comparison of the cyclic voltammogram of (DPAP)Ru^{II}(CO)(DPP) with those of $(DPAP)_2Ru^{II}$-(DPP) and (MeOH)Ru^{II}(CO)(DPP) reveals the existence of an equilibrium between the three species. The anodic peak at $E^{\circ\prime} = +0.49$ V is the only one which can clearly be ascribed to the oxidation of (DPAP)Ru^{II}(CO)(DPP). In contrast, the second peak ($E^{\circ\prime} = +1.00$ V) is not unambiguously attributable. This redox peak probably arises from the overlap of three oxidation processes, in that the process for (DPAP)Ru^{II}(CO)(DPP) is found at the same potential values of the oxidation of $[(DPAP)_2Ru^{II}(DPP)]^+$ and of $[Ru^{II}(CO)$-(DPP)$]^+$, and could hide the expected oxidation of $[(DPAP)$-$Ru^{II}(CO)(DPP)]^+$. A hypothetical mechanism derived by electrochemical analysis involves the loss of the carbonyl

(16) Juris, A.; Prodi, L. *New J. Chem.* **2001**, *25*, 1132.
(17) Mealli, C.; Proserpio, D. M. *J. Chem. Educ.* **1990**, *67*, 399.
(18) Vela, A.; Gazquez, J. L. *J. Phys. Chem.* **1988**, *92*, 5688.
(19) (a) For Ru: Thorn, D. L.; Hoffmann, R. *Inorg. Chem.* **1978**, *17*, 126. (b) For C, H, N: Hoffmann, R. *J. Chem. Phys.* **1963**, *39*, 1397. (c) For P: Summerville, R. H.; Hoffmann, R. *J. Am. Chem. Soc.* **1976**, *98*, 7240.

Table 1. Formal Electrode Potentials (V vs SCE) in CH_2Cl_2 Solution for the Redox Processes of the Ru(II)−Porphyrin Complexes

complex		oxidations		reductions	
		$E^{\circ\prime}_{2+/+}$	$E^{\circ\prime}_{+/0}$	E_p[a]	
$(PR_3)Ru^{II}(CO)(DPP)$	$(MeOH)Ru^{II}(CO)(DPP)$	+1.00	+0.61	−1.8	
	$(DPPA)Ru^{II}(CO)(DPP)$	+0.98[a]	+0.48		
	$(DPAP)Ru^{II}(CO)(DPP)$	+1.02	+0.49		−2.0
	$[(PA)_3P]Ru^{II}(CO)(DPP)$	+1.05	+0.51		−1.9
	$[(PAP(OEt)_2]Ru^{II}(CO)(DPP)$	+0.97	+0.42	−1.8	−2.0
$(PR_3)_2Ru^{II}(DPP)$	$(DPPA)_2Ru^{II}(DPP)$	+1.21	+0.93[a]	+0.09	
	$(DPAP)_2Ru^{II}(DPP)$		+0.95	+0.06	
	$[(PA)_3P)_2]Ru^{II}(DPP)$		+0.94	+0.25	
	$[PAP(OEt)_2]_2Ru^{II}(DPP)$		+0.82	+0.11	

[a] Redox potential values for irreversible processes; measured at 0.2 V s^{-1}.

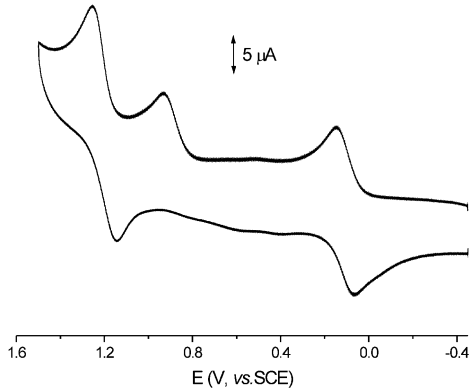

Figure 2. Cyclic voltammetric response recorded at platinum electrode in CH_2Cl_2 solution of $(DPPA)_2Ru^{II}(DPP)$ (0.3×10^{-3} mol dm^{-3}): $[NBu_4][PF_6]$ (0.2 mol dm^{-3}) supporting electrolyte; scan rate 0.2 V s^{-1}.

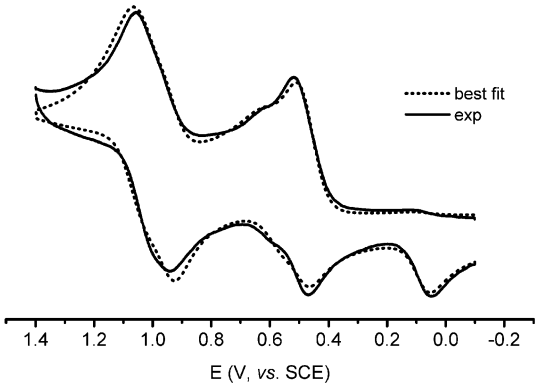

Figure 3. Simulation of the cyclic voltammogram of $(DPAP)Ru^{II}(CO)(DPP)$. The solid line represents the experimental curve, and the dotted line refers to the best fitting; scan rate 0.2 V s^{-1}.

followed by the addition of a second phosphine ligand by the cation $[(DPAP)Ru^{II}(CO)(DPP)]^+$. An analogous process was found to occur in solution upon solvent evaporation.[2] To deconvolute the cyclic voltammogram, we carried out a simulation[20] by considering the presence of three possible chemical processes accompanying the two one-electron removals:

K_1 $Ru^{II}(CO)(DPP) + DPAP \leftrightarrows (DPAP)Ru^{II}(CO)(DPP)$

K_A $(DPAP)Ru^{II}(CO)(DPP) + DPAP \leftrightarrows (DPAP)_2Ru^{II}(DPP) + CO$

K_B $[(DPAP)Ru^{II}(CO)(DPP)]^+ + DPAP \leftrightarrows [(DPAP)_2Ru^{II}(DPP)]^+ + CO$

The experimental voltammogram of $(DPAP)Ru^{II}(CO)(DPP)$, together with the best fit, is shown in Figure 3, while the relative parameters are collected in Table 2. As deducible from Figure 3, the simulated voltammogram nicely agrees with the experimental data. Remarkably, we obtained the same value for K_1 (1.27×10^6 M^{-1}) as obtained by UV−vis spectroscopy ($1.2 \pm 0.3 \times 10^6$ M^{-1}.)[2] The best fit data support the occurrence of two subsequent oxidation processes at +0.49 and at +0.97 V, respectively.

In conclusion, we observe that in the mono-phosphine complexes, the first oxidation is cathodically shifted by 0.1−0.2 V with respect to $(MeOH)Ru^{II}(CO)(DPP)$, while the second oxidation occurs at substantially the same potential values. In contrast, in the bis-phosphine complexes the first oxidation is strongly cathodically shifted (by 0.35−0.55 V) with respect to $(MeOH)Ru^{II}(CO)(DPP)$. Again, the second oxidation is much less affected by the presence of the two axial ligands (less than 0.1 V, an exception being the complex $[PAP(OEt)_2]_2Ru^{II}(DPP)$ with a cathodic shift of 0.18 V). The nature of the redox processes described above will be further discussed in the section devoted to EHMO calculations.

Photophysical Properties. The photophysical data are summarized in Table 3. As can be seen, the maxima of both the B and the Q absorption bands of the monophosphine complexes are very similar to one another, and all are red-shifted compared to $(MeOH)Ru^{II}(CO)(DPP)$ by ca. 10 nm (Figure 4). This behavior is identical to that observed for other $(L)Ru^{II}(CO)(por)$ complexes, where L could be a ligand having either a nitrogen or a phosphorus donor atom.[7,9,21] As was already observed for these complexes, the nature of the ligand L among the same series of complexes has only a small effect on the position of the absorption bands centered on the porphyrin macrocycle.[7] More significant changes, however, are observed on going to the bis-phosphorus complexes. In these cases, a larger red shift of the B band can be observed, while in the 480−600 nm region only one band is generally detected. While the former effect is typically observed when the CO ligand is substituted by a ligand having either a nitrogen or a phosphorus atom,[7,9,21] the second effect on the Q-band absorptions is usually observed only when the Ru(II) center is oxidized to Ru(III).[22] The sharp and well-resolved resonances in both the proton and the phosphorus NMR spectra of all the bis-phosphine

(20) Rudolph, M.; Feldberg, S. W. *DigiSim 3.0 ed.*; Bioanalytical Systems Inc.: Congleton, Cheshire, U.K., 2000.
(21) Tait, C. D.; Holten, D.; Barley, M. H.; Dolphin, D.; James, B. R. *J. Am. Chem. Soc.* **1985**, *107*, 1930.

Table 2. Experimental Data and Best Fit Parameters for the Cyclic Voltammogram Exhibited by a CH_2Cl_2 Solution Containing Equimolar Amounts of $(MeOH)Ru^{II}(CO)(DPP)$ and DPAP (0.1×10^{-3} mol dm^{-3})

parameter	calcd	exptl
$E^{\circ\prime}$ $[Ru(CO)(DPP)]^{2+}/[Ru(CO)(DPP)]^{+}$	+0.98 V	+1.00 V
$E^{\circ\prime}$ $[Ru(CO)(DPP)]^{+}/Ru(CO)(DPP)$	+0.60 V	+0.61 V
$E^{\circ\prime}$ $[(DPAP)_2Ru(DPP)]^{2+}/[(DPAP)_2Ru\ (DPP)]^{+}$	+0.99 V	+0.95 V
$E^{\circ\prime}$ $[(DPAP)_2Ru\ (DPP)]^{+}/(DPAP)_2Ru\ (DPP)$	+0.08 V	+0.06 V
$E^{\circ\prime}$ $[(DPAP)Ru(CO)(DPP)]^{2+}/[(DPAP)Ru(CO)(DPP)]^{+}$	+0.97 V	+1.02 V
$E^{\circ\prime}$ $[(DPAP)Ru(CO)(DPP)]^{+}/(DPAP)Ru(CO)(DPP)$	+0.49 V	+0.49 V
K_1	1.3×10^6 M^{-1}	$1.2 \pm 0.3 \times 10^6$ M^{-1}
K_A	1.33×10^9	
K_B	135	
std deviation	2.8×10^{-7}	

Table 3. Luminescence Data of the Mono-Phosphine and Phosphonite Complexes in CH_2Cl_2 Solutions at 77 K

ligand	λ_{max}/nm	τ/μs
OMe	674	215
$PAP(OEt)_2$	695	240
$(PA)_3P$	697	165
DPAP	701	150
DPPA	702	155

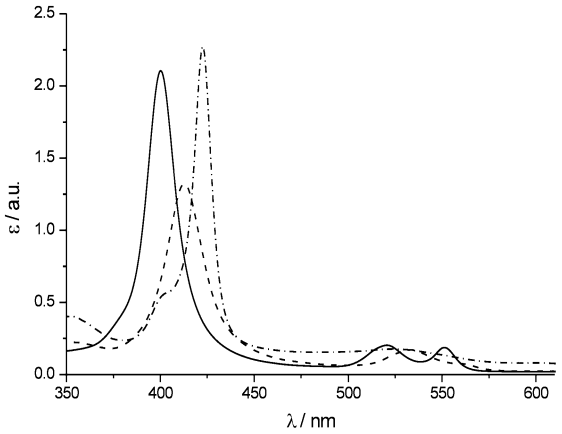

Figure 4. UV−vis spectra of $(MeOH)Ru^{II}(CO)(DPP)$ (—), $(DPAP)Ru^{II}(CO)(DPP)$ (---), and $(DPAP)_2Ru^{II}(DPP)$ (-·-·) in CH_2Cl_2, $c = 1 \times 10^{-4}$ M.

complexes, however, do not support oxidation of the metal.[2] This would lead to a paramagnetic species, inducing severe line broadening in the NMR spectra. In our case, the observed band is probably due to the overlap of different electronic transitions, involving not only the porphyrin macrocycle but also the phosphorus ligands. This interpretation is supported by EHMO calculations (vide infra).

As far as the luminescence is concerned, the spectra of the mono-phosphine and phosphonite complexes in dichloromethane at 77 K are shown in Figure 5. The quite intense luminescence of $(PR_3)Ru^{II}(CO)(DPP)$ can be attributed to originate from a $^3(\pi,\pi^*)$ excited state, in agreement with literature reports for similar complexes with OEP and TPP.[7,9,21] The coordination of the phosphorus ligand leads to a red shift of the phosphorescence band for all the complexes, analogously to the absorption transitions. Among our series, again only relatively small changes in the spectra

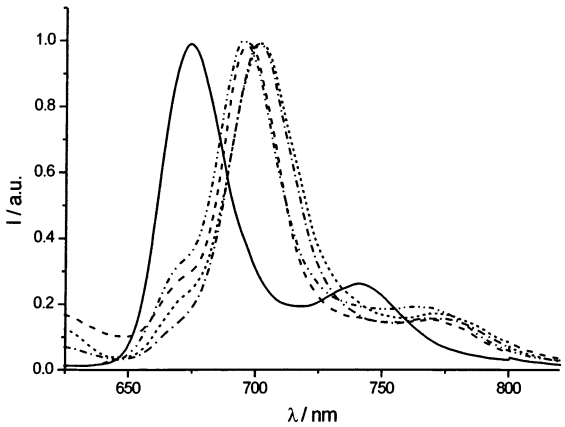

Figure 5. Luminescence spectra of the mono-phosphine and phosphonite complexes $(MeOH)Ru^{II}(CO)(DPP)$ (—), $[PAP(OEt_2)]_2Ru^{II}(DPP)$ (-··-··), $[(PA)_3P]_2Ru^{II}(DPP)$ (---), $(DPPA)_2Ru^{II}(DPP)$ (···), and $(DPAP)_2Ru^{II}(DPP)$ (-·-·). Spectra are recorded in CH_2Cl_2 solution at 77 K.

occur in the $(PR_3)Ru^{II}(CO)(DPP)$ complexes as the sixth ligand L is varied, as it has been observed for a series having nitrogen as donor atom.[7] From the structure of the band, and from the relatively long excited state lifetime (hundreds of microseconds), the luminescence of the monophosphine complexes can also be attributed to a $^3(\pi,\pi^*)$ state. [7,9,21]

As was found for the absorption properties, replacement of the CO ligand with another phosphorus ligand leads to dramatic changes in the photophysical properties of the complexes, and in particular to the complete quenching of the luminescence. Typically, in the complexes of the kind $(PR_3)_2Ru^{II}(DPP)$, the absence of the strong $d\pi \rightarrow CO(\pi^*)$ back-bonding present in the $(PR_3)Ru^{II}(CO)(DPP)$ complexes increases the energy of the $d\pi$ orbitals centered on the metal. As a result, in these complexes the lowest excited state of the systems is a (d,π^*) metal to porphyrin charge-transfer state.[21] This excited state is typically nonluminescent and exhibits lifetimes on the order of tens of nanoseconds. In addition, in the bis-phosphorus complexes reported here, a charge-transfer state involving the phosphorus ligands could also occur at low energy, as suggested by EHMO calculations. This additional excited state is also expected to be nonluminescent, in agreement with the observed behavior.

EHMO Calculations. EHMO calculations were performed to establish how the nature of the axial ligands affects the energy of the frontier orbitals. A fragment analysis method was used to elucidate the interaction between the fragment $Ru^{II}(DPP)$ and the different pair of axial ligands. Figure 6 gives an overall picture of the main differences in

(22) (a) Ariel, S.; Dolphin, D.; Domazetis, G.; James, B. R.; Leung, T. W.; Rettig, S. J.; Trotter, J.; Williams, G. M. *Can. J. Chem.* **1984**, *62*, 755. (b) Barley, M.; Becker, J. Y.; Domazetis, G.; Dolphin, D.; James, B. R. *Can. J. Chem.* **1983**, *61*, 2389.
(23) Cambridge Crystallographic Data Centre (CCDC), 12 Union Road, Cambridge CB2 1EZ, UK

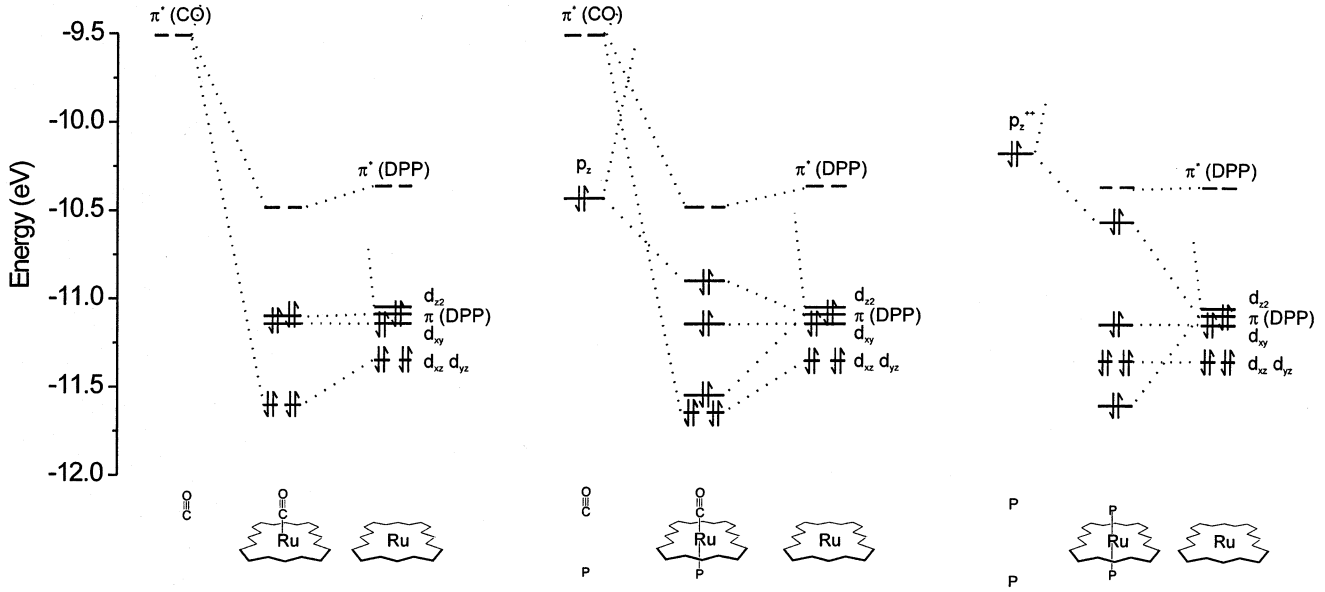

Figure 6. Fragment interaction diagram for $Ru^{II}(CO)(DPP)$, $(PR_3)Ru^{II}(CO)(DPP)$, and $(PR_3)_2Ru^{II}(DPP)$ complexes.

the fragment interaction diagram of $Ru^{II}(CO)(DPP)$, (PR_3)-$Ru^{II}(CO)(DPP)$, and $(PR_3)_2Ru^{II}(DPP)$.

The HOMO of the $Ru^{II}(CO)(DPP)$ complex is a porphyrin-centered π orbital, derived from the delocalized porphyrin core. The orbital immediately lower in energy is the nonbonding ruthenium d_{xy} orbital, which cannot interact with the carbonyl π^* by back-bonding effects like d_{xz} and d_{yz}. Indeed, d_{xz} and d_{yz} are found lower in energy.

The HOMO in the mono-phosphine species $(PR_3)Ru^{II}$-$(CO)(DPP)$ and in the bis-phosphine complexes $(PR_3)_2Ru^{II}$-(DPP) derive from the antibonding interaction between the p_z axial phosphorus atom orbital and the π porphyrin orbital. This p_z is also stabilized to some extent by the ruthenium d_{z^2} orbital. As a result, in the mono-phosphine species (PR_3)-$Ru^{II}(CO)(DPP)$ the main contribution to the HOMO arises from the π porphyrin system, while in the bis-phosphine complex $(PR_3)_2Ru^{II}(DPP)$ the HOMO is much higher in energy and mainly localized on the two axial phosphorus atoms.

In all cases, the HOMO-1 is the nonbonding ruthenium d_{xy}, which remains unaffected in energy regardless of the ligands on the ruthenium center. The d_{xz} and d_{yz} orbitals are strongly influenced by the presence or absence of CO due to stabilizing π-back-bonding effects. Lack of these effects in the $(PR_3)_2Ru^{II}(DPP)$ complexes effectively reverses the relative order for the lower lying orbitals.

In agreement with the experimental results, the first oxidation process, which involves the removal of one electron from the π-system of the porphyrin core or from the phosphine ligands, is expected to occur at more positive potentials according to the order $(PR_3)_2Ru^{II}(DPP) < (PR_3)$-$Ru^{II}(CO)(DPP) < Ru^{II}(CO)(DPP)$. In addition, the second oxidation process, involving the removal of one electron from the ruthenium d_{xy}, orbital is expected to occur at the same potential values for all the complexes.

The EHMO calculations show that the LUMO is a porphyrin-centered π^* orbital; its energy is slightly stabilized by a contribution of the $\pi^*(CO)$ orbital. Indeed, in the case of $(PR_3)_2Ru^{II}(DPP)$ complexes the LUMO is higher in energy. The experimental data concerning the reduction processes apparently do not match the EHMO calculations. Experimentally, the peak potential values shift toward more cathodic values on going from $(MeOH)Ru^{II}(CO)(DPP)$ to $(PR_3)Ru^{II}(CO)(DPP)$, a change that is not reproduced by the theoretical calculations. We must, however, consider that the irreversibility of the reduction processes causes loss of their thermodynamic meaning.

Conclusions

The design of large porphyrin assemblies has become a major field of research, mainly because of the attractive photophysical and electrochemical properties of the porphyrin unit. In the design of large porphyrin assemblies, great care has to be taken in the choice of the different building blocks in order to obtain a directional energy or electron transfer from one porphyrin unit to the adjacent porphyrin. In particular, if energy transfer is envisaged, the use of bis-phosphine ruthenium(II) complexes should be avoided, since their efficient deactivation to the ground state could prevent the desired transfer processes inside the assembly. On the other hand, interesting properties are shown by the mono-phosphine complexes, which could be inserted at the periphery of the assembly. The photophysical and electrochemical data reported here are then essential for the choice of the different components, in order to have energy- or electron-migration in the correct direction. It is, however, notable that the differences in the stereoelectronic properties of the various phosphorus ligands studied here do not have a significant influence on the photophysical and electrochemical properties of the ruthenium(II) porphyrin.

Acknowledgment. Financial support is acknowledged from the Swiss National Science Foundation (Grant 8220-061293) for E.S. and MURST (Artifical Photosynthesis and

Solid Supermolecules Projects) for L.P. P.Z. gratefully acknowledges the financial support of the University of Siena (PAR 2001); P.Z. and E.G. acknowledge CIRCMSB for a one-year scholarship. Careful revision of the manuscript by Amy L. Kieran is very much appreciated.

IC025728Q